JOURNAL OF SOLID STATE CHEMISTRY 1, 545–553 (1970)

Mixed Oxides of the Type MO_2(Fluorite)-M_2O_3. V. Phase Studies in the Systems ZrO_2–M_2O_3 (M = Sc, Yb, Er, Dy)†‡

M. R. THORNBER

Division of Applied Mineralogy, C.S.I.R.O., Wembley, Western Australia

D. J. M. BEVAN AND E. SUMMERVILLE

School of Physical Sciences, The Flinders University of South Australia, Bedford Park, South Australia

Received September 10, 1969

Results of phase studies on the systems ZrO_2–M_2O_3 (M = Sc, Yb, Er, Dy) are reported. Room-temperature X-ray diffraction of quenched and annealed samples is the main technique used, and the difficulties inherent in this approach to the determination of phase equilibria are discussed. Many of the data so obtained probably relate to metastable states, the nature of which is discussed in the light of structural information on ordered intermediate phases in the ZrO_2–Sc_2O_3 and ZrO_2–Yb_2O_3 systems. Some speculations on the question of the stability and structure of grossly nonstoichiometric phases observed in various composition regions of these systems are made.

Introduction

There is now sufficient structural information on fluorite-related ordered intermediate phases of the systems ZrO_2–M_2O_3 (M = Sc, rare-earth metals) to attempt a description of the phase relationships observed in these systems (which may not, and often do not, represent the equilibrium situation) in terms of structural features derived from the ordered phases. This paper reports the results of some detailed phase studies of the systems. ZrO_2–Sc_2O_3, ZrO_2–Yb_2O_3, ZrO_2–Er_2O_3, and ZrO_2–Dy_2O_3 in which room-temperature powder X-ray diffraction data have been obtained for numerous samples as a function of composition and heat treatment.

† Part I. Oxygen Dissociation Pressures and Phase Relationships in the System CeO_2–Ce_2O_3 at High Temperatures (*1*).

Part II. Non-Stoichiometry in Ternary Rare-Earth Oxide Systems

A. The System CeO_2–Y_2O_3.

B. The Systems CeO_2–M_2O_3 (M = La,Nd,Sm,Gd,Dy,Ho,Yb) (*2*).

Part III. Crystal Structures of the Intermediate Phases $Zr_5Sc_2O_{13}$ and $Zr_3Sc_4O_{12}$ (*3*).

Part IV. *J. Solid State Chem.*, preceding paper.

‡ This work was carried out in the School of Chemistry, University of Western Australia.

Methods and Limitations

There are two major problems in a study of this kind, bearing in mind that the ultimate aim is to deduce the equilibrium T–X phase relationships in the subsolidus region:

(i) How can the samples best be prepared so that equilibrium can be achieved in the heat treatment?

(ii) How can room-temperature X-ray data be related to the situation (hopefully equilibrium) obtaining at elevated temperatures? This implies the need to know what processes occur during cooling.

Any attempt to quench the high-temperature situation is unlikely to be completely successful: the oxygen sublattice in these fluorite-related systems is far too mobile. By contrast, the diffusion data given in Table I suggest that below 1000°C the metal atoms are likely to be so immobile as to preclude the achievement of equilibrium in any reasonable time, particularly where phase reactions occur.

The samples were prepared either by physical mixing of the component oxides or by coprecipitation of the oxide hydrates. Heat treatment of samples prepared by the first method may result in spontaneous chemical diffusion processes leading to what must be a lower free-energy state and may be the

TABLE I

DIFFUSION COEFFICIENTS FOR OXYGEN AND ZIRCONIUM AT VARYING TEMPERATURES

	Oxygen Diffusion in β-Phase Zirconia-Scandia[a]		Oxygen Diffusion in Calcia Stabilized Zirconia (*5*)		Zirconium Diffusion in Calcia Stabilized Zirconia (*6*)	
Temp °C	D cms²/sec	$\sqrt{6 \times D}$[b] Å	D cms²/sec	$\sqrt{6 \times D}$[b] Å	D cms²/sec	$\sqrt{6 \times D}$[b] Å
400	1×10^{-11}	7.8×10^{2}	1.6×10^{-12}	3.1×10^{2}	2×10^{-32}	3.5×10^{-8}
560	6×10^{-10}	6×10^{3}	1.1×10^{-10}	2.6×10^{3}	2×10^{-26}	3.5×10^{-5}
727	4×10^{-8}	5×10^{4}	2.5×10^{-9}	1.2×10^{4}	2×10^{-22}	3.5×10^{-3}
977	7×10^{-7}	2×10^{5}	6.0×10^{-8}	6×10^{4}	2×10^{-18}	0.35
1394	2×10^{-6}	3.5×10^{5}	1.4×10^{-6}	2.9×10^{5}	2.5×10^{-14}	35

[a] Calculated from the conductivity data of Strickler and Carlson (*4*) using the Nernst–Einstein relationship and assuming a transport number of 1 for oxygen.

[b] $\sqrt{6 \times D}$ = the root mean square of the distance travelled by the average atom in one second for a cubic material.

equilibrium state, but the time for complete reaction to occur, especially at low temperatures, may be very large. The difficulty is then to extrapolate from data on incompletely reacted specimens.

Those samples prepared by coprecipitation already have the components intimately mixed, usually in a metastable state, and these must then unmix; in doing so, other metastable states are apt to result. In spite of these limitations, however, useful information can be obtained.

The heat treatments used in this work ranged from the melting of samples in an argon arc to long anneals (~ 100 days) in air at temperatures below 1000°C. Both Hägg–Guinier and Debye–Scherrer powder cameras were used to obtain the X-ray diffraction patterns.

Results and Discussion

The System ZrO_2–Sc_2O_3

This was first studied by Lefèvre (*7*) and is the only one of the four discussed here which has been widely studied. A composite phase diagram is shown in Fig. 1, constructed from the results of Lefèvre, Strickler and Carlson (*8*), Domagala (*9*), Ruh (*10*), and the present work. It is an attempt to rationalize the evidence available and to take cognisance of the fact that many of the data reported are from quenched samples. It must, however, be very tentative. The most significant feature is the existence at room temperature of the three ordered intermediate phases β, γ, and δ (Lefèvre's designation). The structures of the last two have now been determined (*3*). Other features of the subsolidus region, although of less significance for the present discussion, are:

(i) The existence at elevated temperatures of a broad, nonstoichiometric, fluorite-type phase (designated α) which extends up to about 27 mole % $ScO_{1.5}$.

(ii) An ill-defined region of tetragonal solid solution (designated T), separated from the α region by a narrow diphasic region. The low-temperature limit of this tetragonal phase is shown as a eutectoid point, but its temperature is uncertain.

(iii) A region of monoclinic solid solution close to the ZrO_2 limit (although it is not yet clearly established that monoclinic ZrO_2 can accommodate Sc_2O_3 in solid solution), and the diphasic regions M + T and M + β.

(iv) A wide diphasic region on the $ScO_{1.5}$-rich side of the diagram between the δ phase and the σ phase.

At low $ScO_{1.5}$ concentration the phase relationships are in some doubt [see (i) and (ii) above], and further work by the present authors is in progress.

Incomplete structural studies on the β phase have suggested that it forms from the disordered, fluorite-type α phase by a disorder → order process in which one of the cubic [111] axes becomes unique, resulting in a complex rhombohedral supercell of probable ideal composition $Zr_{48}Sc_{14}O_{117}$. The dimensions of the triply primitive hexagonal cell are $a = 19.80(1)$ Å, $c = 17.99(6)$ Å. The structure is closely related to fluorite, and probably occurs

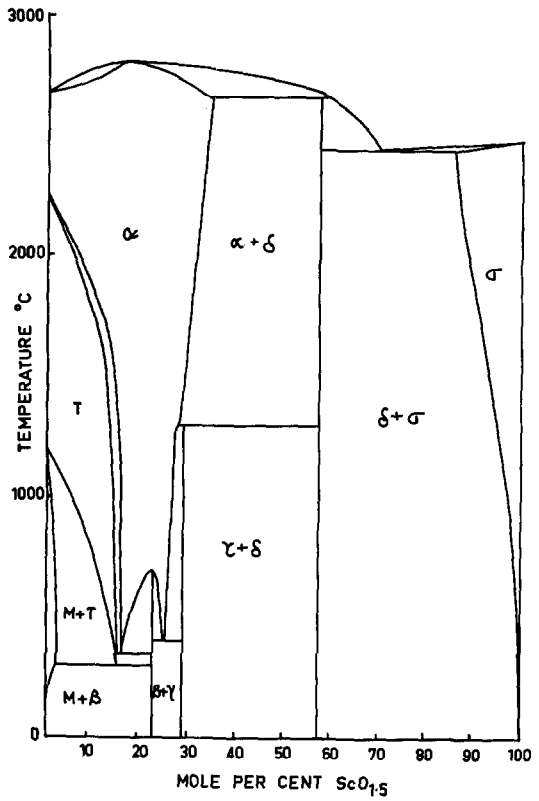

FIG. 1.

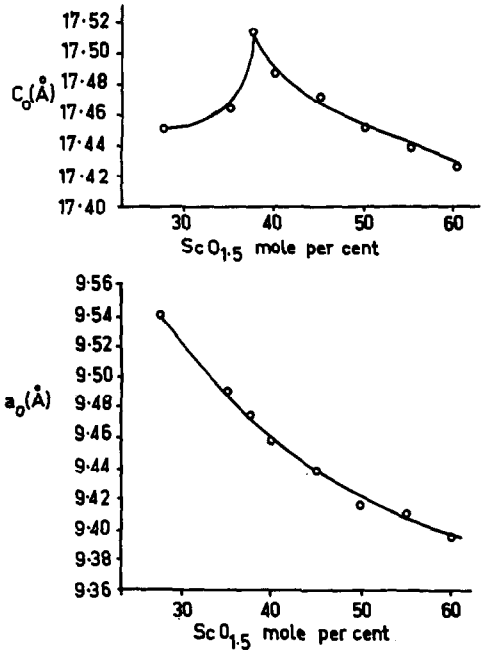

FIG. 2.

in the $R3$ space group. If the composition is as given above, the β phase cannot have *vacancy pairs* as in the γ and δ phases (*3*), and a new *vacancy* ordering principle must apply. All samples of this phase, studied by X-ray diffraction and optical and electron microscopy, show multiple twinning on a very fine scale with the twin boundaries parallel to (001) cubic planes. The twins are related by a 180° rotation about any one of the three [110] cubic directions that are perpendicular to the unique [111] cubic axis which has become the hexagonal c direction. Further work is in progress.

In Fig. 1 the β, γ, and δ phases are shown as line phases, in apparent contradiction to the findings of previous workers and, indeed, to some results obtained in the present study. This requires some comment. In this work, samples in the $\gamma + \delta$ region, prepared by coprecipitation of the hydrated oxides and subsequent heat treatment at about 1600°C, gave diffraction patterns which clearly indicated the presence of two phases ($\gamma + \delta$) of essentially unvarying composition. By contrast, samples which had been melted in an argon arc and cooled rapidly on the water-cooled copper hearth gave monophasic rhombohedral diffraction patterns which showed many of the characteristic features of either γ or δ depending on the composition. Superficially, they constitute evidence for a continuous transition between the two at high temperatures, in general agreement with the conclusions reached by others. These patterns were indexed satisfactorily on the basis of a γ-type unit cell, and Fig. 2 shows the variation of the hexagonal a and c parameters with composition across the range: a transforms smoothly but there is an apparent discontinuity in c at 37.5 mole % $ScO_{1.5}$ which is not explained. However, when these samples were annealed at 1600°C (the highest annealing temperatures available) separation into the two phases occurred, and it is possible that the monophasic quenched melt is metastable with respect to a diphasic equilibrium as shown in Fig. 1. More careful study is needed before this issue can be resolved. In the phase diagram as sketched, the equilibrium situation at 1600°C is described by a diphasic equilibrium, α (of composition close to the γ-phase composition) + δ, and the appearance of γ at room temperature implies the rapid conversion of α to γ.

In this context the structural studies on γ and δ (*3*) are relevant. These have shown that the cation sublattices are randomly populated by Zr and Sc atoms, and only the vacancy pairs in the oxygen sublattice are ordered, this ordering leading to the

rhombohedral distortion of what is essentially a complete fluorite-type array of metal atoms. Moreover, this vacancy pair ordering is extremely rapid—a quenched melt of composition corresponding to that of either γ or δ gives a perfect γ or δ diffraction pattern. The monophasic rhombohedral patterns from quenched melts of intermediate compositions may therefore only indicate the formation on solidification of a single, continuous, fluorite-type cation sublattice, and an oxygen sublattice within which the vacancy pairs are aligned along one of the cubic [111] directions and so distributed as to constitute what can be described as a *pseudo phase* consisting of microdomains of γ and δ, coherent or at least semi-coherent one with the other. To achieve a diphasic equilibrium state a phase reaction involving considerable cation redistribution must occur, and this bulk diffusion of cations in fluorite-type structures is well-known to be very sluggish except at high temperatures.

A similar argument applies where the β phase is concerned. This has been reported to have quite a wide homogeneity range, but the difficulty of achieving equilibrium in phase reactions below about 600°C, the upper temperature limit of existence of this phase, is very great.

Formation of such pseudophases in phase reactions, where the structures of the two phases coexisting at equilibrium are closely related, has been studied in some detail for the systems $PrO_x + O_2$ (*11*) and $TbO_x + O_2$ (*12*). It occurs only when the direction of reaction is towards greater order, and is associated with hysteresis and it seems to be particularly prevalent when fluorite-related structures are involved. In such systems, then, if intermediate phases exist at all, they are more likely to be line phases *at equilibrium* than phases of broad compositional width. It is another problem to determine the temperatures at which such phases disorder, and whether this occurs by congruent or incongruent melting, peritectoid reaction, or order–disorder transformation.

The Systems ZrO_2–M_2O_3 (M = Yb, Er, and Dy)

Previous work in this area has been carried out by Collongues and his colleagues (*7*), (*13*), and (*14*), and more recently by Rouanet (*15*). The phase $Zr_3Yb_4O_{12}$ was discovered by the French group, and the structures of the two modifications are described in the preceding paper. In all these systems an α phase is a dominant feature. In reports of the earlier work, mention is made of the occurrence of complicated hexagonal phases at high M_2O_3 content: these are not mentioned by Rouanet, and in the present work the X-ray diffraction lines ascribed to them were not observed when the rare-earth oxide starting materials were first purified by dissolution and homogeneous precipitation of the metal ions in acid solution by dimethyl oxalate. The choice of these systems for detailed study in conjunction with the studies on the system ZrO_2–Sc_2O_3 was dictated by Collongues' observation that the phase relationships were very dependent on the ionic radius of the rare-earth cation [cation radii (*16*); $Zr^{4+} = 0.79$ Å, $Sc^{3+} = 0.81$ Å, $Yb^{3+} = 0.86$ Å, $Er^{3+} = 0.89$ Å, $Dy^{3+} = 0.92$ Å].

This previous work on the ZrO_2–M_2O_3 systems was carried out at temperatures above 1200°C, whereas in the binary rare-earth oxide systems the ordered phases form at temperatures of 1000°C and below. Sawyer et al., (*17*) found that annealing of samples of the ordered PrO_x phases at temperatures as low as 400°C produced sharp X-ray patterns. Accordingly, a series of samples in the systems ZrO_2–$YbO_{1.5}$ and ZrO_2–$DyO_{1.5}$ were prepared (by coprecipitation) in the composition range (15–60 mole % $MO_{1.5}$) where ordered phases are found in the binary systems, and these were heated at 1150°C, then gradually annealed down to room-temperature over 27 days in the hope of producing ordered phases. All samples showed a well-formed α-type phase. If the formation of ordered phases required ordering of the oxygen sublattice only, then presumably such phases would have formed. This result indicates that ordering of the metal atoms is required, which is in accord with what has been postulated by workers on the binary systems (*17*) and the structural evidence on the low-temperature form of $Zr_3Yb_4O_{12}$ (see previous paper).

Another series of compositions in the system ZrO_2–$DyO_{1.5}$ was prepared by physical admixture of the oxide powders in the required proportions. The following heat treatments were given in succession, the samples being investigated after each treatment:

1. Heated at 1050°C for 20 days.
2. Heated at 1350°C for 5 days.
3. Annealed from 1250–1000°C over 90 days.

Table II gives the phases present in each sample and the unit cell volume of any phase, where measurable, after the first heat treatment. While there was still some unreacted ZrO_2 and $DyO_{1.5}$ present, there were also two distinct α phases, α_1 and α_2, in most samples. From the cell volumes the compositions of these phases could be estimated. The expected feature, if complete solid solution were to exist at

TABLE II
INTERPRETATION OF X-RAY PATTERNS OF PHYSICAL MIXTURES OF ZrO_2 AND $DyO_{1.5}$ AFTER HEATING AT 1050°C FOR 20 days

Prepared Composition mole % $DyO_{1.5}$	Phases Present in Order of X-Ray Intensity Plus Unit Cell Volume (Å^3) where Measured		
100	$DyO_{1.5}$ (151.7)		
90	$DyO_{1.5}$ (151.7)	α_1	α_2
80	$DyO_{1.5}$ (151.7)	α_1 (138.3)	α_2 (144.6)
57.2	$DyO_{1.5}$ (151.7)	α_1 (138.2)	α_2 (144.2)
53.5	$DyO_{1.5}$ (151.7)	α_1 (138.2)	α_2 (143.4)
44.4	α_1 (138.0)	$DyO_{1.5}$ (151.7)	α_2 (142.9)
35.0	α_1 (138.1)	$DyO_{1.5}$ (151.7)	α_2 —
29.0	α_1 (diffuse) (138)	$DyO_{1.5}$ (151.7)	ZrO_2 —
20.0	α_1 (137.4)	ZrO_2 —	$DyO_{1.5}$ (151.7)
10.0	α_1 (137.1)	ZrO_2 —	$DyO_{1.5}$ —

this temperature, would have been one α-type phase, identifiable by a very diffuse X-ray pattern as the two oxides diffused into each other and a variety of compositions formed. An interesting feature is that no σ-type phase was produced. Thus, it would seem that C-type $DyO_{1.5}$ coexists with the α_2 phase at these temperatures. The α_2 phase and α_1 phase can exist together, and the α_1 phase with monoclinic ZrO_2. Comparison of the cell volumes of the α_1 and α_2 phases with data from fully reacted samples of known composition places the α_1 composition range from 21–29% $DyO_{1.5}$ and the α_2 range from 53–59% $DyO_{1.5}$, which encompasses the 57.14% of a δ-type phase.

After further heating at 1350°C for 5 days, poorly crystallized but single α phases were formed, whose parameters corresponded to those obtained from coprecipitated samples. Compositions at 80 and 90% $DyO_{1.5}$ gave a diffuse σ-type phase plus a very sharp α pattern which corresponded to the α_2 region. Indications are that at 1350°C the miscibility gap between α_1 and α_2 is closed and that α_2 coexists with a σ phase of composition 85% $DyO_{1.5}$.

Annealing of these samples at 1250°C, and then down to 1000°C over 90 days did not alter the powder patterns to any marked degree. Thus, unmixing into separate phases may be very difficult to achieve.

Figure 3 shows a plot of unit cell volume versus composition for the systems ZrO_2–$DyO_{1.5}$, ZrO_2–$ErO_{1.5}$, and ZrO_2–$YbO_{1.5}$. The black spots are representative of samples that have been heated at 1600°C prior to measurement. Open circles represent samples that have been annealed at temperatures lower than 1600°C. In some cases, particularly in the ZrO_2–$DyO_{1.5}$ system where there are more data, a degree of unmixing is indicated. However, once samples had been fired at temperatures greater than 1450°C, very little could be done by way of annealing at lower temperatures to alter the well-crystallized fluorite-type α phase (20–60% $MO_{1.5}$) which was formed. In the ZrO_2–Yb_2O_3 system the α phase extended only to ~ 50 mole % $YbO_{1.5}$, and the ordered phase $Zr_3Yb_4O_{12}$ was formed at 57.14 mole % $YbO_{1.5}$.

The two-phase region separating the α region (δ phase for the ZrO_2–$YbO_{1.5}$ system) from the σ region is quite clearly delineated. This was not observed in Rouanet's work on quenched samples where he indicates a continuous transition from α to σ.

For each system there are three lines drawn through the black spots: a line from 20–33% $MO_{1.5}$, referred to as the α_1 region; a line from 33–60% $MO_{1.5}$ called the α_2 region; a line at high $MO_{1.5}$ content in the σ-phase region. These lines have all been calculated by least-squares methods, and the respective linear equations are listed in Table III. Each point falls well within experimental error of its particular line.

Kempter (*18*) has emphasized that variations of unit-cell parameter with composition are more truly represented by the Zen relationship than by the better known Vegard's "law" (*19*). The Zen relationship (*20*) can be represented by

$$V = V_1 - (V_1 - V_2)X$$

where

V = unit cell volume of the solid solution

V_1 = unit cell volume of component 1

V_2 = unit cell volume of component 2

X = mole fraction of component 2.

In Figure 3 there are three linear relationships for each system. Comparing the equations of these lines (Table III) with the Zen relationship, values for V_1 and V_2 can easily be calculated and these are listed in Table IV. The Zen relationship can now

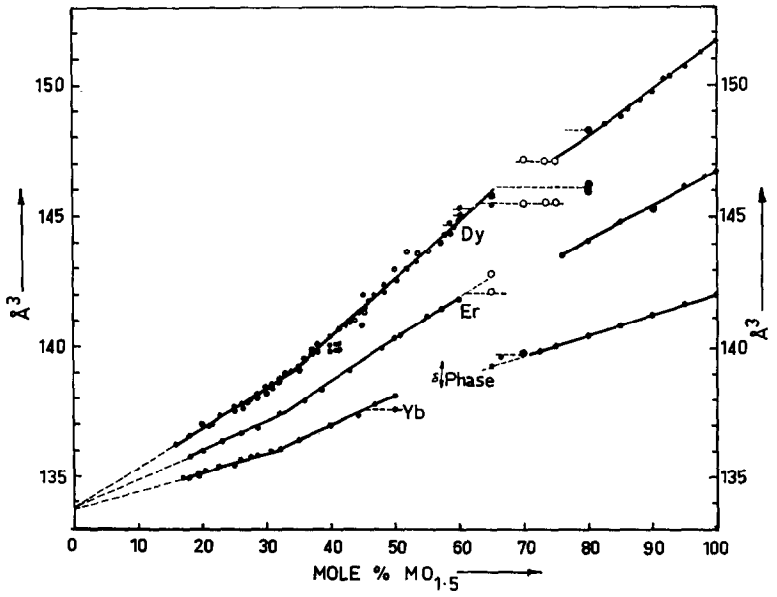

FIG. 3.

TABLE III

EQUATIONS OF LINES SHOWN IN FIGURE 3

Equations are of the Form, Vol = $V_1 + B$ (mole % $MO_{1.5}$), and Standard Deviation = s.d.

	α_1 region			α_2 region			σ region		
$MO_{1.5}$	V_1	B	s.d.	V_1	B	s.d.	V_1	B	s.d.
$DyO_{1.5}$	133.88	0.15022	0.07	131.60	0.21937	0.08	133.22	0.18464	0.07
$ErO_{1.5}$	133.75	0.11298	0.04	132.12	0.16302	0.07	133.68	0.13042	0.05
$YbO_{1.5}$	133.63	0.07792	0.06	132.70	0.10738	0.06	134.18	0.07857	0.04

TABLE IV

VOLUMES V_1 AND V_2 COMPUTED FROM THE EQUATIONS IN TABLE III ON THE BASIS OF THE ZEN RELATIONSHIP $V = V_1 - (V_1 - V_2)X$

(Units are in Å^3.)

	α_1 Region		α_2 Region		σ Region	
$MO_{1.5}$	V_1	V_2	V_1	V_2	V_1	V_2
$DyO_{1.5}$	133.88	148.90	131.60	153.54	133.22	151.68
$ErO_{1.5}$	133.75	145.05	132.12	148.42	133.68	146.72
$YbO_{1.5}$	133.63	141.42	132.70	143.44	134.18	142.04

be used in reverse. V_1 is an estimation of the volume contribution of ZrO_2 to the volume of a unit cell of the solid solution in that region: V_2 is the volume contribution of the particular rare-earth oxide. It is easily seen from Table IV that this effective volume of $ZrO_2(V_1)$ for the α_1 region of the three systems is essentially the same if due regard is taken for the errors incorporated in extrapolating the line of best fit to the ZrO_2 axis. This suggests the occurrence of Zr atoms in a similar environment

throughout this composition range for all three systems. The volume contributions (V_2) of the rare-earth oxides in this region are also consistent, but the values are substantially less than the comparable unit cell volumes of the pure oxides.

For the α_2 region the effective volume of ZrO_2(V_1) is again almost the same from one system to the next, but is markedly smaller than V_1 for the α_1 region. By contrast, V_2 values have increased and are now above those for the pure oxides. Qualitatively these observations constitute clear evidence that the environments of both Zr and M atoms are different in the two regions α_1 and α_2. More specifically, they suggest that in the α_2 region the drop in V_1 is due to a decrease of oxygen coordination around Zr atoms which stems from the preferential coordination by Zr of the vacancy pair, as revealed by the structural studies on the low-temperature form of $Zr_3Yb_4O_{12}$, and that the increase in V_2 is due to a concomitant increase in the oxygen coordination of M atoms. The additional fact that V_1 in this α_2 region increases slightly as the size of the M cation is decreased, is an indication that the distinction by oxygen atoms between the small Zr^{4+} and somewhat larger M^{3+} ions is made less readily as the sizes become more nearly equal and the preference for Zr to be 6-coordinated becomes less marked; again in accord with the structural observations. At the δ-phase composition in the ZrO_2–Er_2O_3 system, samples annealed at 1000°C after heating at 1600°C contained a second minor phase, seen under the polarising microscope as small optically-active crystals in an isotropic matrix. Long exposure brought up a weak sharp superstructure in the X-ray powder pattern which indexed on the basis of a δ-type unit cell of hexagonal dimensions $a = 9.70(7)$ Å $c = 9.08(3)$ Å. Table V shows the indexing of this phase, presumed to be $Zr_3Er_4O_{12}$, which has been able to nucleate but not to grow to any size due to a strict requirement for cation ordering.

A δ-$Zr_3Dy_4O_{12}$ phase has not been seen. The large size variation between a Zr^{4+} ion and a Dy^{3+} ion probably means that its formation would require complete metal ordering, but the low metal diffusion rates preclude this. Evidence from the physically mixed samples suggests that δ-$Zr_3Dy_4O_{12}$ may exist but only ordered to very short range. In fact this whole α_2 region may be a disordered δ-type phase.

The σ phase for all systems extends from 100% to near 70% $MO_{1.5}$ for samples heated at 1600°C. For samples annealed at lower temperatures the composition range of the σ phase is reduced and the diphasic region between σ and α_2 (δ for the ZrO_2–$YbO_{1.5}$ system) is correspondingly increased. Figure 3 shows linear plots of 1/8 of the body-centred unit cell volume versus composition for the three systems. Equations of these lines and values of V_1 and V_2, are listed in Tables III and IV, respectively. The V_2 values are of course the volumes

TABLE V

INDEXING OF δ-PHASE $Zr_3Er_4O_{12}$

SHARP SUPERSTRUCTURE LINES WHICH BECAME APPARENT ONLY AFTER LONG EXPOSURE OF CUBIC PHASE

Intensity	$h\,k\,l$	$\sin^2\theta$ Observed	$\sin^2\theta$ Calculated
VW	1 1 0	0.02511	0.02519
Cubic 111 VVS and broad	0 0 3	0.06560	0.06473
	2 1 1		0.06596
Cubic 200 VVS and broad	2 1 2	0.08752	0.08753
W	1 1 3	0.08991	0.08991
W	3 1 1	0.11623	0.11633
W	1 0 4	0.12342	0.12347
W	3 1 2	0.13806	0.13791
W	3 0 3	0.14020	0.14029
W	4 0 1	0.14131	0.14152
W	4 0 2	0.16273	0.16309
Cubic 220 VVS and broad	2 1 4	0.17501	0.17384
MW	4 1 0	0.17629	0.17630
MW broad	3 2 2	0.18825	0.18828
	1 0 5		0.18820
W	3 1 4	0.22439	0.22421
Cubic 311 VS and broad	2 1 5	0.24103	0.23857
	4 1 3		0.24103
	4 2 1		0.24225
W	4 0 4	0.24928	0.24940
MW	0 0 6	0.25948	0.25892
Cubic 222 VS	—	0.26215	—
M	4 2 2	0.26340	0.26383
W	5 1 1	0.26685	0.26744
W	1 1 6	0.28421	0.28410
W	5 1 2	0.28900	0.28902
	3 1 5		0.28894
VW	5 2 0	0.32739	0.32741
W	4 3 2	0.33963	0.33939
	3 2 5		0.33931
Cubic 400 VS	4 2 4	0.34966	0.35014
W	6 0 3	0.36697	0.36696
W	5 2 3	0.39218	0.39214
MW diffuse	2 1 7	0.41189	0.41118
Cubic 331 VS	4 2 5	0.41526	0.41487
MW	7 0 1	0.41839	0.41856
	5 3 1		0.41856
Cubic 420 VS	4 1 6	0.43709	0.43521
M diffuse	7 0 2	0.44008	0.44013
	5 3 2		0.44013
	5 1 5		0.44005

of the C-type oxides. The V_1 values are not accurate as they have resulted from a long extrapolation, but even so they are very consistent for the three systems and similar to V_1 for the α_1 region. This suggests that the environment of the Zr atoms is similar here and in the α_1 region where they are probably either 7- or 8-coordinated. Thus, it can be inferred that in the σ phase the extra oxygen atoms, which occupy interstitial sites in the C-type matrix of 6-coordinated metal atoms, are coordinating Zr atoms. This is in contrast with the preferential coordination of the vacancy pairs by Zr atoms for the neighbouring α_2 region, and is consistent with the observation that a miscibility gap always separates these α_2 and σ regions.

General Discussion

From the present study of the systems ZrO_2–$MO_{1.5}$ (M = Dy, Er, and Yb) no real understanding of the *equilibrium* phase relationships can be established. This is due to the inability to quench in the true high-temperature situation with any certainty because of the extremely mobile oxygen atoms. At the same time the low diffusion rates of the metal atoms prevent the true equilibrium situation from being obtained at low temperature by annealing procedures.

No indication of cation ordering or site preference of metal atoms has been found in the ZrO_2–$ScO_{1.5}$ system, and the structural data from this system may be regarded as showing qualitatively how the oxygen atoms and vacancies would be arranged if an ordered metal-atom arrangement could be achieved. The region in this system from $MO_{1.85}$ to $MO_{1.714}$, where the oxygen vacancies are in pairs across the body diagonal of a cube coordinating a metal atom, covers the same composition range in which, at low temperatures, the ordered binary phases of the homologous series M_nO_{2n-2} occur. It is also the same composition range where the α_2 type of disordered phase has been observed for the systems ZrO_2–$MO_{1.5}$ (M = Yb, Er, and Dy), and it may be inferred that this vacancy pair type of short-range order is the controlling feature in this region. Furthermore, the structural evidence from studies of $Zr_3Yb_4O_{12}$ shows that there is a preference for the smaller, 4-valent metal atom to coordinate the vacancy pair, and if the difference in size between Zr^{4+} and Yb^{3+} can be considered as sufficient to result in cation ordering in the low-temperature $Zr_3Yb_4O_{12}$, then it may be expected that the even larger size variation between the +3 and +4 metal ions in the binary systems would require ordering of the metal lattice to be a necessary feature of these systems, an ordering which in these cases, however, is readily achieved by electron switching.

Evidence has been put forward to show that the α_1 and α_2 regions of the disordered ternary systems are quite distinct, although the X-ray patterns for both phases appear to be fluorite. The α_1 region in the ZrO_2–$MO_{1.5}$ (M = Dy, Er, Yb) systems covers a similar composition range to the α-phase region of the ZrO_2–$ScO_{1.5}$ system, and this α phase orders up rapidly at low temperatures to form the β phase. Structural studies on the β phase have shown that the type of ordering is distinct from that in any ordered phase occurring in other systems in the α_2 composition range, and the solution of the structure of the β phase may reveal the key to the short-range order of the α_1 region and show why it should be distinct from the α_2 region.

It may even be the case that both these α_1 and α_2 regions, formed at high temperature, are metastable with respect to diphasic equilibria as in the ZrO_2–$ScO_{1.5}$ case, and that the recorded observations, made at room temperature on *quenched* specimens, are indicative of incipient unmixing into ordered intermediate phases (of microdomain dimensions?) at least semicoherent with the matrix.

Acknowledgments

The authors express their gratitude to Drs. B. G. Hyde and L. A. Bursill for assistance in establishing the twinning relationships in the β phase by electron microscopy and diffraction, and to the Australian Atomic Energy Commission for financial support under Contract 65/K/4.

References

1. D. J. M. Bevan and J. Kordis, *J. Inorg. Nucl. Chem.* **69**, 480 (1964).
2. D. J. M. Bevan, W. W. Barker, R. L. Martin, and T. C. Parks, "Rare Earth Research," (L. Eyring, Ed.), Vol. 3, p. 441, Gordon and Breach, New York, (1965).
3. M. R. Thornber, D. J. M. Bevan, and J. Graham, *Acta Cryst.* **B24**, 1183 (1968).
4. D. W. Strickler and W. G. Carlson, Westinghouse Research Laboratories, Scientific Paper 64-918-273, p. 2, 1964.
5. L. A. Simpson and R. E. Carter, *J. Amer. Ceram. Soc.* **49**, 139 (1966).
6. W. H. Rhodes and R. E. Carter, *J. Amer. Ceram. Soc.* **49**, 244 (1966).
7. J. Lefèvre, *Ann. Chim.* **8**, 117 (1963).
8. D. W. Strickler and W. G. Carlson, Westinghouse Research Laboratories, Report 63-943-267, p. 4, 1963.
9. R. F. Domagala, "A Study of the Zirconia-Scandia System," Aerospace Research Laboratories, 66-0230 (1966).
10. R. Ruh, American Ceramic Soc. Meeting, 1967.

11. B. G. HYDE, D. J. M. BEVAN, AND L. EYRING, *Phil. Trans. Roy. Soc. A*, **259**, 583 (1966).
12. B. G. HYDE AND L. EYRING "Rare Earth Research," Vol. 3, p. 623, Gordon and Breach, New York, 1965.
13. M. PEREZ Y JORBA, *Ann. Chim.* **7**, 479 (1962).
14. R. COLLONGUES, F. QUEYROUX, M. PEREZ Y JORBA, AND J-C. GILLES, *Bull. Soc. Chim. France* 1141 (1965).
15. A. ROUANET, *Compt. Rend.* **267**, 1581 (1968).
16. L. H. AHRENS, *Geochim. Cosmochim. Acta* **2**, 155 (1952).
17. J. O. SAWYER, B. G. HYDE, AND L. EYRING, *Bull. Soc. Chim. France* 1190 (1965).
18. C. P. KEMPTER, *Phys. Status Solidi* **18**, K117 (1966).
19. L. VEGARD, *Z. Phys.* **5**, 17 (1921).
20. E. ZEN, *Amer. Mineral.* **41**, 523 (1956).